Tectonics Modulated Long-Term Weathering Inputs From the East Asian Continent and Tropical Island Arc to the South China Sea Since the Late Oligocene

Mengjun Li, Christophe Colin, Shiming Wan, Zhaojie Yu, Zhimin Jian, Zehua Song, Arnaud Dapoigny, Hualong Jin, Jin Zhang, Debo Zhao, et al.

Geophysical Research Letters

RESEARCH LETTER
10.1029/2024GL114500

Tectonics Modulated Long-Term Weathering Inputs From the East Asian Continent and Tropical Island Arc to the South China Sea Since the Late Oligocene

Mengjun Li[1,2], Christophe Colin[3], Shiming Wan[1,2], Zhaojie Yu[1,2], Zhimin Jian[4], Zehua Song[1], Arnaud Dapoigny[5], Hualong Jin[1], Jin Zhang[1], Debo Zhao[1], and Anchun Li[1]

[1]Key Laboratory of Marine Geology and Environment, Institute of Oceanology, Chinese Academy of Sciences, Qingdao, China, [2]Laboratory for Marine Geology, Qingdao Marine Science and Technology Center, Qingdao, China, [3]Université Paris–Saclay, CNRS, GEOPS, Orsay, France, [4]State Key Laboratory of Marine Geology, Tongji University, Shanghai, China, [5]Laboratoire des Sciences du Climat et de l'Environnement, LSCE/IPSL, CEA–CNRS–UVSQ, Université Paris–Saclay, Gif–sur–Yvette, France

Abstract The chemical weathering of Earth's silicate rocks regulates the global climate. However, the exact role of continental weathering with orogenic building and island arc weathering with arc-continent collisions remains unclear. Here, we established a seawater neodymium isotopic composition (ε_{Nd}) record for the northern South China Sea (SCS) since 28 Ma, retrieving from planktonic foraminifera at International Ocean Discovery Program Site U1501. The progressively restricted SCS connection from the Pacific Ocean and intensified weathering inputs from the East Asian Continent correspond to an unradiogenic trend of ε_{Nd} records between 17 and 9 Ma. The radiogenic trend of ε_{Nd} records since 9 Ma could be induced by enhanced tropical island arc weathering inputs in the context of the Luzon Arc-Eurasian Continent collision, which resulted in significant atmospheric CO_2 consumption. This study highlights that enhanced weathering of tropical island arc potentially significantly contributed to global cooling since the late Miocene.

Plain Language Summary Silicate weathering of continents and island arcs are key processes in impacting the Earth's climate through removing CO_2 from the atmosphere. However, the exact roles of these two weathering systems during different geological periods remain poorly understood. This study presents new seawater neodymium isotopic records in the northern South China Sea (SCS) since 28 Ma. These seawater fingerprints could examine the evolution of weathering inputs from East Asian continental rocks and tropical volcanic island arc that have influenced the northern SCS since the late Oligocene. Between 17 and 9 Ma, the unradiogenic trend of ε_{Nd} values indicates the gradual isolation of the SCS basin and intensified weathering inputs from the East Asian Continent. In contrast, the more radiogenic trend in ε_{Nd} values since 9 Ma, corresponds to the collision of the Luzon Arc and the Eurasian Continent during this period, which led to rapid weathering of the tropical island arc. The enhanced weathering of the tropical island arc could have increased CO_2 consumption, potentially contributing to global cooling. These findings highlight the important role of tropical volcanic island arc in climate regulation and provide new insights into how tectonic evolution has shaped the seawater Nd isotopic composition in the deep SCS basin.

Key Points:

- First planktonic foraminiferal Nd isotopic record in the South China Sea since the late Oligocene was established
- Enhanced weathering inputs from the Asian Continent led to an unradiogenic trend of ε_{Nd} records between 17 and 9 Ma
- Radiogenic trend of ε_{Nd} since 9 Ma indicates increased tropical island arc weathering due to the Luzon Arc-Eurasian Continent collision

Supporting Information:

Supporting Information may be found in the online version of this article.

Correspondence to:

S. Wan and Z. Yu,
wanshiming@ms.qdio.ac.cn;
yuzhaojie@qdio.ac.cn

Citation:

Li, M., Colin, C., Wan, S., Yu, Z., Jian, Z., Song, Z., et al. (2025). Tectonics modulated long-term weathering inputs from the East Asian Continent and tropical island arc to the South China Sea since the late Oligocene. *Geophysical Research Letters*, *52*, e2024GL114500. https://doi.org/10.1029/2024GL114500

Received 9 JAN 2025
Accepted 17 APR 2025

Author Contributions:

Conceptualization: Shiming Wan
Data curation: Mengjun Li, Shiming Wan
Formal analysis: Mengjun Li, Christophe Colin, Shiming Wan, Zhaojie Yu, Zhimin Jian, Zehua Song, Arnaud Dapoigny, Hualong Jin, Jin Zhang, Debo Zhao
Funding acquisition: Shiming Wan
Investigation: Mengjun Li, Shiming Wan
Methodology: Mengjun Li, Christophe Colin, Shiming Wan, Arnaud Dapoigny
Project administration: Shiming Wan
Resources: Christophe Colin, Shiming Wan, Anchun Li

1. Introduction

The Earth's cooling trend during the Cenozoic has been primarily attributed to several key processes: reduced volcanic outgassing (Herbert et al., 2022), the burial of organic carbon on continental margins (Galy et al., 2007), and enhanced silicate weathering in the Himalayas and Tibetan Plateau, which sequesters carbon dioxide (CO_2) through carbonate precipitation in the ocean (Raymo & Ruddiman, 1992; Song et al., 2023). Recently, it has been hypothesized that arc-continent collisions in the tropics could be responsible for CO_2 depletion and glaciations by rapidly exhuming and eroding mafic and ultramafic rocks within large volcanic island arcs (Bayon et al., 2023; Jagoutz et al., 2016; Macdonald et al., 2019). However, the silicate weathering processes induced by the uplift of volcanic island arcs and the Himalayas-Tibetan Plateau have not been independently recorded in a certain area (Jagoutz et al., 2016), a fact that prevents us from identifying the dominant role of volcanic arcs and crustal continent rocks in the weathering to the ocean, especially since the late Cenozoic.

Software: Mengjun Li
Supervision: Shiming Wan, Anchun Li
Validation: Mengjun Li, Christophe Colin, Shiming Wan
Visualization: Mengjun Li, Shiming Wan
Writing – original draft: Mengjun Li, Shiming Wan
Writing – review & editing: Mengjun Li, Christophe Colin, Shiming Wan, Zhaojie Yu, Zhimin Jian

The dissolved neodymium isotopic composition ($^{143}Nd/^{144}Nd$) of seawater, expressed as ε_{Nd}, is not homogeneous in oceans because of its residence time (~500–1,000 years) (Siddall et al., 2008; Tachikawa et al., 2003) being shorter than the mean mixing time of the global ocean (~1,500 years) (Piepgras & Wasserburg, 1982). Seawater ε_{Nd} records are considered as quasi-conservative tracers for fingerprinting the evolution of deep-water masses characterized by different isotopic compositions in the geological past (e.g., Colin et al., 2019; Dubois-Dauphin et al., 2017; Piepgras & Wasserburg, 1982). However, the ε_{Nd} values of water masses can also be modified by discharges of freshwater and sediments from rivers (Burton & Vance, 2000; Yu et al., 2017), by "boundary exchange" corresponding to the exchange of Nd between water masses and sediments deposited on oceanic margins (Jeandel et al., 2007; Lacan & Jeandel, 2005; Lacan et al., 2012), and/or the benthic flux from pore water in certain oceanic areas (Abbott et al., 2015). These processes are particularly well pronounced in marginal seas under the influence of large sediment inputs, such as in the Bay of Bengal (Singh et al., 2012; Song et al., 2023; Yu et al., 2017) and the South China Sea (SCS) (Wu et al., 2017).

At modern times, the SCS is a semi-enclosed marginal sea connected to the western Pacific Ocean through the Luzon Strait at a modern sill depth of ~2,400 m, which is the only passage for the Pacific Ocean deep-water masses (North Pacific Deep Water, NPDW; Upper and Lower Circumpolar Deep Water, UCDW and LCDW) to enter the SCS (Qu et al., 2006; Wyrtki, 1961). The SCS receives a large amount of suspended sediments (approximately 700 million tons annually) from surrounding drainage basins (e.g., the Pearl River, the Red River and the Mekong River), representing 3.7% of the estimated global fluvial sediment discharge into the world's oceans (Milliman & Farnsworth, 2011). Given that the ε_{Nd} values of these riverine sediments are markedly more unradiogenic (ε_{Nd} values from −13 to −11) (Wei et al., 2012) than those of Pacific Ocean deep-water masses that enter the SCS via the Luzon Strait (ε_{Nd} values of −4 to −2.5 for NPDW; ε_{Nd} values of −9 to −6 for LCDW/UCDW) (Amakawa et al., 2019; Wu et al., 2015), the SCS is an ideal setting for evaluating the influence of lithogenic Nd inputs from these large Asian rivers. In addition, seawater ε_{Nd} has been recognized as a sensitive tracer of the weathering of volcanic island arcs and the partial dissolution of volcanogenic particles, both of which are characterized by radiogenic Nd isotopic compositions (Bayon et al., 2023; Wu et al., 2017). These signals with more radiogenic ε_{Nd} values from the weathering of volcanic island arcs: ε_{Nd} values from +2 to +8 for volcanic rocks in the Philippine Islands (Sajona et al., 2000; Solidum et al., 2003); ε_{Nd} values from +6.5 to +7.1 for stream sediments on Luzon Island (Goldstein & Jacobsen, 1988) and ε_{Nd} values from −3.7 to +5.3 for sediments offshore of the southern Philippines Arc in the western Pacific (Wei et al., 2012). These sediments can be transported to the deep SCS basin by the intruding Pacific Deep Water (PDW) (Wu et al., 2017).

The ε_{Nd} values of planktonic foraminifera have been shown to reflect the Nd isotopic composition of bottom water and/or porewater rather than ambient seawater at calcification depths, as element Nd is mainly hosted and concentrated by Fe-Mn oxyhydroxide coatings formed after deposition at the sediment-seawater interface (Piotrowski et al., 2012; Tachikawa et al., 2014). Furthermore, the signal of ε_{Nd} reflects the integrated weathering inputs and represents a denudation flux that integrates both physical erosion and chemical weathering processes (Bayon et al., 2023; Yu et al., 2018). In this study, we analyzed the ε_{Nd} values of mixed planktonic foraminifera from International Ocean Discovery Program (IODP) Site U1501, located on the northern margin of the SCS, to establish the past Nd isotopic composition of deep water and the long-term evolution of weathering inputs. Overall, our new results make it possible to assess the relative contribution from crustal continents (i.e., the East Asian Continent) and the western Pacific island arcs to weathering inputs, which are closely linked to regional tectonic evolution over time.

2. Materials and Methods

Drilling at IODP Site U1501 (18°53.09′N, 115°45.95′E, water depth of 2,846 m; Figure 1) on the northern SCS has recovered a continuous deep-sea sedimentary record of terrestrial erosion in South China since the Eocene (Jian et al., 2018, 2019; Jin et al., 2022). The age model for Site U1501 has been well established using biostratigraphic data (calcareous nannofossils and planktonic foraminifera), magnetostratigraphic data and $^{87}Sr/^{86}Sr$ ratios of foraminifera shells (Figure 2) (Jian et al., 2018, 2019). For this study, we investigated the upper 300 mbsf (meters below the sea floor) of the sedimentary sequence over the last 28 Ma.

About 30 mg of well-preserved mixed species planktonic foraminifera were measured from 68 samples at the *Géosciences Paris–Saclay* laboratory at the *University Paris–Saclay*. After cleaning and weak acid leaching, we follow the method outlined by Copard et al. (2010) for Nd purification. The $^{143}Nd/^{144}Nd$ ratios were analyzed

10.1029/2024GL114500

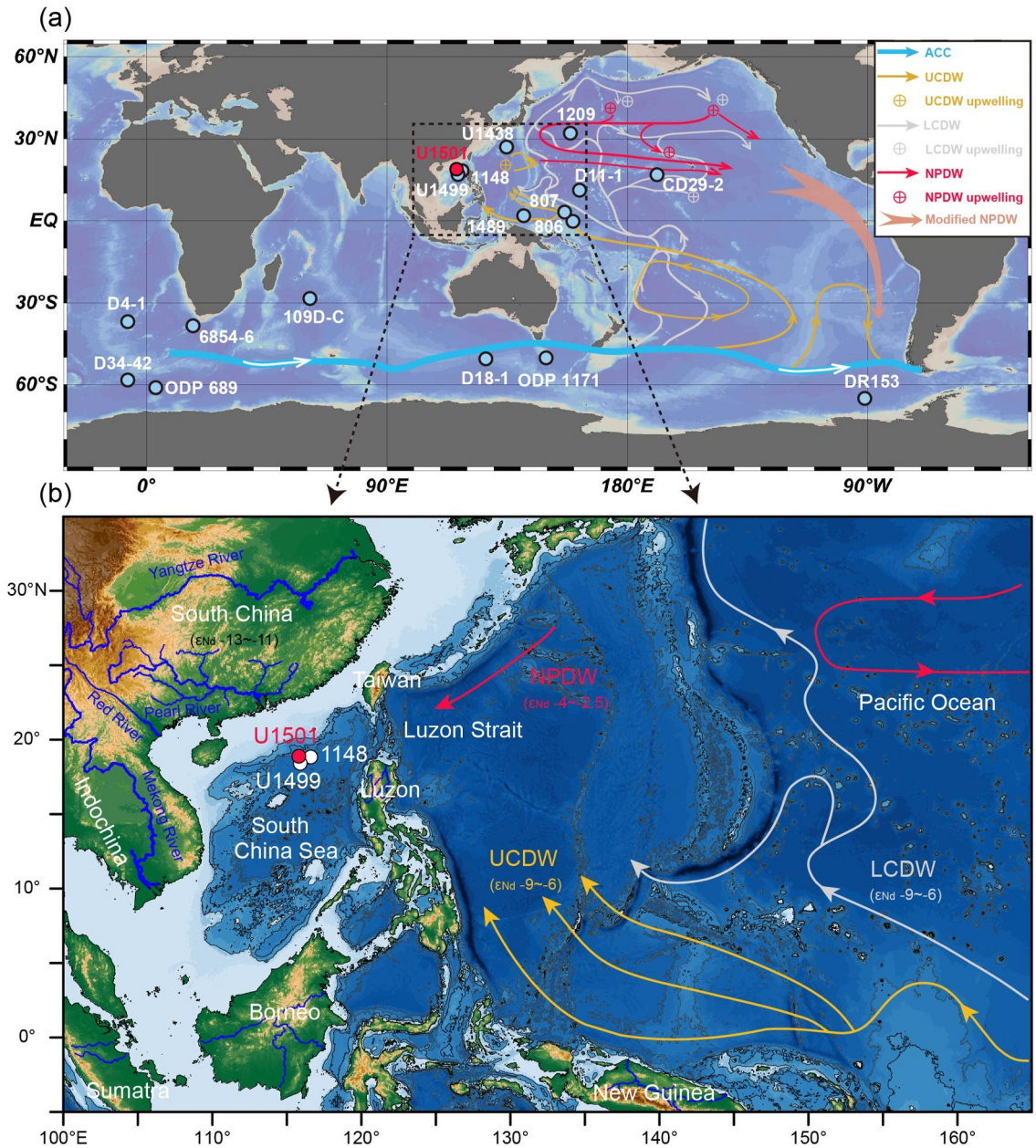

Figure 1. (a) Location map showing available seawater ε_{Nd} records from the Southern Ocean (Frank et al., 2002; Holbourn et al., 2013; Scher & Martin, 2004), the equatorial-north Pacific Ocean (Holbourn et al., 2013; Jian et al., 2023; Kender et al., 2018; Le Houedec et al., 2016; Ling et al., 1997; McKinley et al., 2019) and the South China Sea (SCS) (Ma et al., 2018; Shu et al., 2024). The map also illustrates modern deep Pacific Ocean circulation (Kawabe & Fujio, 2010), including Antarctic Circumpolar Current, Lower and Upper Circumpolar Deep Water (LCDW and UCDW), and North Pacific Deep Water (NPDW) (details in Text S1 in Supporting Information S1); (b) Regional map depicting the locations of International Ocean Discovery Program Sites U1501 and U1499, ODP Site 1148 in the northern SCS. The map also highlights major river drainage systems and the modern schematic pathways of LCDW, UCDW and NPDW.

using the *Thermo Fisher Neptune*^{Plus} Multi–collector Inductively Coupled Plasma Mass Spectrometer (MC–ICP–MS) hosted at *the Laboratoire des Sciences du Climat et de l'Environnement (LSCE)*, France. During the analytical sessions, every three samples were bracketed using JNdi–1 Nd standard solutions (Tanaka et al., 2000) (Details are presented in Text S2 in Supporting Information S1).

10.1029/2024GL114500

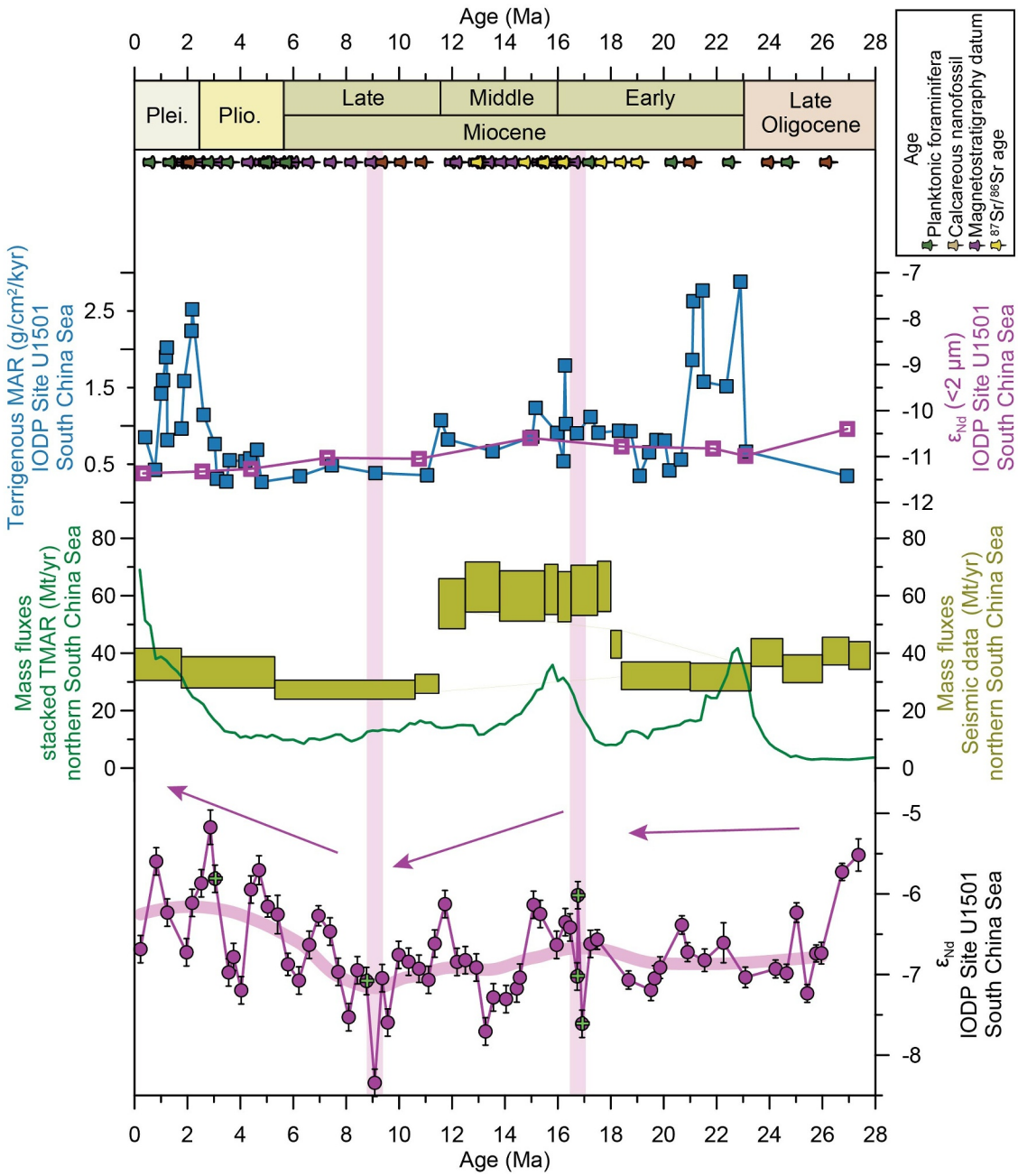

Figure 2. Variations in ε_{Nd} values of planktonic foraminifera and detrital fraction, terrigenous mass accumulation rates (TMARs, g/cm^2/kyr) at International Ocean Discovery Program Site U1501 since 28 Ma. The reconstruction of mass fluxes based on stacked TMAR records from multiple sites and seismic data in the northern South China Sea is also shown (Clift, 2006; Jin et al., 2023). The green cross symbols on the ε_{Nd} plot represent key transition points, calculated by the first derivative. The pink band represents the LOESS smoothing. Bold pink lines indicate periods of significant variation in ε_{Nd} values.

3. Results

The ε_{Nd} values obtained from samples of mixed planktonic foraminifera collected from Site U1501 exhibit large variations, with an amplitude of approximately 3.6 epsilon units (ranging from -8.3 ± 0.17 to -4.7 ± 0.15) since 28 Ma (Figure 2 and Data Set S1). The long-term variations in the foraminiferal ε_{Nd} record reveal an initial excursion toward less radiogenic ε_{Nd} values of approximately two epsilon units around 28 and 26 Ma. This shift is followed by long-lasting negative shifts in ε_{Nd} values, persisting from 26 to 17 Ma (slightly down to lower values reaching −7.6) and then from 17 to 9 Ma (markedly down to lower values reaching −8.3). In contrast, after 9 Ma,

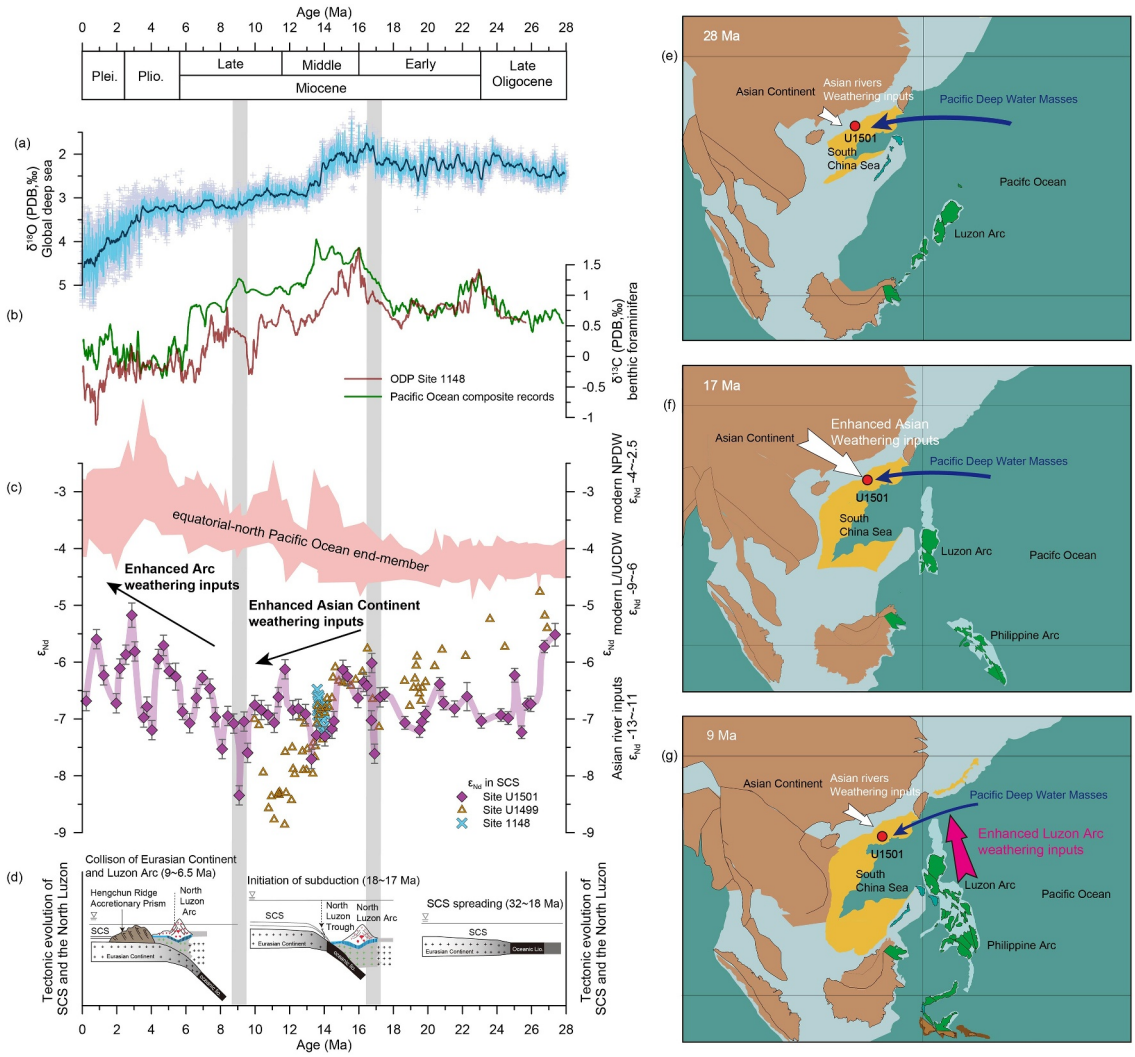

Figure 3. Temporal variations in seawater ε_{Nd} values, climate change and tectonic evolution of the South China Sea (SCS) and the Luzon Arc since the late Oligocene. (a) Marine benthic $\delta^{18}O$ (Westerhold et al., 2020); (b) Benthic foraminifera $\delta^{13}C$ at ODP Site 1148 and Pacific Ocean composite records (Chen et al., 2015); (c) Comparison of ε_{Nd} values Sites U1501, U1499 (Shu et al., 2024) and 1148 (Ma et al., 2018), and the equatorial-north Pacific Ocean end-member (details are presented in Figure S1 in Supporting Information S1); (d) Main tectonic evolution in the SCS and the North Luzon Arc (Hall, 2002; Huang et al., 2018); Schematic diagram illustrating the paleogeographic reconstructions and weathering inputs from the East Asian Continent and the Luzon Arc at (e) 28 Ma, (f) 17 Ma, and (g) 9 Ma (after Hall, 2002).

the ε_{Nd} record toward a more radiogenic value of more than three epsilon units (Figure 2). Notably, the amplitudes of ε_{Nd} variation become more pronounced between 9 and 3 Ma, characterized by peaks of increasingly radiogenic values (Figure 2). The ε_{Nd} records of fish teeth from Sites U1499 (Shu et al., 2024) and 1148 (Ma et al., 2018), both located proximate to Site U1501, exhibit similar ranges to those at Site U1501 between 27 and 10 Ma (Figure 3c), indicating that ε_{Nd} values at Site U1501 reliably reflect the local bottom water signal.

4. Discussion

The Nd isotopic composition of foraminifera at Site U1501 (ε_{Nd} values from −8.3 to −4.7) represents a mixture of signals from lithogenic Nd derived from river sediments around the SCS (ε_{Nd} values, −13 to −11) and intruded PDW masses, NPDW (ε_{Nd} values of −4 to −2.5) and UCDW and/or LCDW (ε_{Nd} values of −9 to −6) (Figure 1) (Kawabe & Fujio, 2010; Wu et al., 2017). Therefore, the long-term variations in foraminiferal ε_{Nd} values at Site U1501 over the last 28 Ma may have resulted from (a) major changes in the sediment provenance due to the reorganization of the main Asian river systems; (b) changes in ε_{Nd} of deep water masses from the Pacific Ocean;

and (c) variations in the relative contributions of lithogenic Nd inputs from crustal rocks located on the western edge of the SCS and from basaltic rocks of island arc along the eastern edge of the SCS. This could provide important clues to evaluate and discuss the reorganization of deep-water circulation in the Pacific, and more importantly, silicate weathering inputs from the East Asian Continent and island arc since the late Oligocene.

The sources of terrigenous sediments on the northwestern SCS have been well constrained by previous studies, which show that the sediments originated dominantly from South China via the Pearl River since the late Oligocene (Clift et al., 2002; Wan et al., 2007). A recent study based on clay minerals and Sr–Nd isotopic compositions of clay-sized sediments from Site U1501 confirmed a consistent sediment source mainly originating from the Pearl River basin since 30 Ma, driven by the uplift of the SE Tibetan Plateau (Jin et al., 2022). Therefore, the foraminiferal ε_{Nd} record cannot be associated with any changes in the provenance of the detrital sediments.

4.1. Impacts of Changes in the ε_{Nd} Values of the PDW and Hydrological Exchanges With the Pacific Ocean

We compiled available seawater Nd isotope ratios from potential end-members (locations of sites and references are shown in Figure 1; records are presented in Figure S1 in Supporting Information S1) to evaluate the impact of bathed water masses. Seawater ε_{Nd} records from the high-latitude Southern Ocean end-member show a relatively stable trend since the late Oligocene (Figure S1 in Supporting Information S1). In contrast, seawater ε_{Nd} records from the equatorial-north Pacific Ocean display an overall increasing trend of ∼4 ε_{Nd} units between 20 and 4 Ma, resulting from the increase in volcanic activities, rapid erosion of radiogenic island arcs and/or reduced entrance of unradiogenic deep-water masses from the Indian Ocean (Figure 3c and Figure S1 in Supporting Information S1) (Bayon et al., 2023; Frank et al., 2002; Kender et al., 2018; Le Houedec et al., 2016; Ling et al., 1997; van de Flierdt et al., 2004).

There is a clear and consistent offset between the ε_{Nd} records of Site U1501 and the equatorial-north Pacific Ocean end-member before 17 Ma (Figure 3c). Between 17 and 9 Ma, seawater ε_{Nd} records from Site U1501 and the equatorial-north Pacific end-member display distinct, almost opposite variations (Figure 3c). This unradiogenic trend is further corroborated by ε_{Nd} values from fossil fish teeth at Site U1499 (water depth of 3,758 m), which show a shift of ∼3 epsilon units between 17 and 10 Ma (Figure 3c) (Shu et al., 2024). A comparison of terrigenous MAR data between Sites U1501 and U1499 reveals a stable pattern, with persistently higher values at Site U1501 between 17 and 11 Ma (Figure S2 in Supporting Information S1). This suggests that Site U1501 with shallower water was more strongly influenced by sediments from continent input, characterized by unradiogenic ε_{Nd} values, during this period. In contrast, ε_{Nd} values at Site U1499 show a more unradiogenic trend over the same period (Figure 3c). This unradiogenic trend at Site U1499 has been attributed to the subsidence and deepening of the SCS basin, allowing more invasion of LCDW (average depths of ∼4,000 m, ε_{Nd} average of −6.4) relative to UCDW (average depths of ∼2,800 m, ε_{Nd} average of −4.5) after 15 Ma (Shu et al., 2024). However, Site U1501 experienced a gradual transition from the outer shelf-upper slope (water depth <1,000 m) during the early Oligocene to a lower slope (∼2,500 m) at 28–24 Ma, eventually reaching its modern depth (∼2,846 m) (Jian et al., 2019). Given the shallower depth, Site U1501 was predominantly influenced by UCDW inflow from the Pacific, with almost no contribution from LCDW. Therefore, the discrepancy in the vertical structure of the water column, bathed at Sites U1501 and U1499, explains the offset in ε_{Nd} values between the two sites.

In the late Oligocene and early Miocene, the deep SCS basin was spreading and largely open to the Pacific Ocean via a large deep strait (Figure 3e) (Hall, 2002; Huang et al., 2018). In such a configuration, the exchange of deep-water masses between the Pacific Ocean and the SCS was strong (Figure 3e). Thus, the variations in ε_{Nd} records from Site U1501 before 17 Ma show small fluctuations, similar to the equatorial-north Pacific Ocean end-member, with slight negative ε_{Nd} shifts due to the proximity of large Asian rivers (Figure 3c).

However, the SCS basin subsequently became progressively more restricted since the middle Miocene (Chen et al., 2015), with reduced water mass intrusion from the Pacific Ocean as a result of (a) the subduction of the SCS oceanic lithosphere eastward beneath the Huatung Basin/Philippine Sea Plate at ∼18–17 Ma and; (b) the development of tectonic-morphological barriers, including the Hengchun Ridge accretionary prism, the Taiwan accretionary prism and the North Luzon Arc at ∼17–16 Ma (Figure 3d) (Huang et al., 2018). This isolation of the deep SCS basin from the Pacific Ocean has been recognized as a primary factor controlling the benthic $\delta^{13}C$ depletion in the SCS relative to those of the Pacific Ocean since 16 Ma (Figure 3b) (Chen et al., 2015). In addition, reconstructions of the terrigenous MAR at Site U1501, mass fluxes based on stacked records and seismic data for the northern SCS (Figure 2) indicate a higher rate of erosion during the early to middle Miocene, resulting from

strong tectonic activity (Clift, 2006; Jin et al., 2023) and enhanced monsoon (Clift et al., 2014). This variation in sediment flux (Figure 2) is almost consistent with the significant shift to more unradiogenic foraminiferal ε_{Nd} values at the study site (Figure 3c). The combined effects of a restricted SCS and increased continental inputs likely explain why ε_{Nd} values at Site U1501 became more unradiogenic, with greater amplitudes of variations after about 17 Ma and up until 9 Ma (Figure 3f).

4.2. Arc-Continent Collision Driven Seawater ε_{Nd} Variations Since the Late Miocene

Afterward, over the last ~9 Ma, the foraminiferal ε_{Nd} record at Site U1501 indicates a shift toward more radiogenic compositions and seems in line with records of the equatorial–north Pacific end–member (Figure 3c). The reduction in Pacific deep–water hydrological exchanges with the deep SCS basin since the middle Miocene (~16 Ma), rules out the increased contribution of PDW masses over the last 9 Ma. In addition, evidence has suggested enhanced aridification of Central Asia and eolian input to the North Pacific at ~9–8 Ma (Shen et al., 2017; Yang et al., 2021), implying dust serves as a potential radiogenic Nd source. However, numerous studies indicate that eolian dust contributed minimally to the northern SCS relative to huge fluvial sediments since the early Miocene (Jin et al., 2022; Liu et al., 2016; Wan et al., 2007). Therefore, dust deposition may have left radiogenic imprints on SCS seawater but insufficiently contributed to the rise in ε_{Nd} values since 9 Ma. The reconstructed terrigenous MAR records from Site U1501 and stacked mass fluxes from the northern SCS (Jin et al., 2023) show a decrease in terrigenous input beginning in the middle Miocene but do not indicate any notable reductions around 9 Ma (Figure 2). These records imply a reduction in unradiogenic lithogenic Nd contributions from Asian river basins since the middle Miocene, however, without a distinct decrease occurred at 9 Ma. Thus, the positive shift in the ε_{Nd} record at Site U1501 after 9 Ma likely reflects a relatively increased contribution of radiogenic Nd in the deep seawaters, related to volcanic island arc inputs at the eastern edge of the SCS.

Various lines of evidence have suggested that arc-continent collision in the tropical SE Pacific since the late Cenozoic accelerated the uplift and exposure of island areas, which in turn enhanced erosional inputs into the ocean (Bayon et al., 2023; Hall, 2002; Molnar & Cronin, 2015). The substantial turbidite sedimentary sequences in the Luzon forearc basin, massive deposition of sediments corresponding to 5–6 km of crust in the Borneo Basin, and extensive sections of forearc basement in Timor since the late Miocene are indicative of these processes (Hall, 2002; Huang et al., 2018). The Luzon Arc consists of a ~1,200 km chain of Miocene to recent stratovolcanoes and volcanic necks, stretching from Mindoro to the coastal range of Taiwan Island (Hall, 2002, 2009). It appears that the initial collision of the North Luzon Arc and the Eurasian Continent began in the latest Miocene (Figure 3d), supported by: (a) reconstruction models (9–6 Ma) (Sibuet et al., 2002; Sibuet & Hsu, 2004); (b) the emergence of the Taiwan accretionary prism (<8.5–6.4 Ma) (Chen et al., 2017); (c) the presence of Taiwan-derived syn-collisional sediments in the forearc basin (6.5 Ma) (Huang et al., 2018; Lin et al., 2003); and (d) older cooling events in the Central Range (7.1 ± 1.3 Ma) (Mesalles et al., 2014).

Given the heavy rainfall in the tropical rain belt (~15°S–20°N) and the steep topography that characterizes the catchment areas of island arcs, there is considerable physical erosion and chemical alteration of the extensive low-latitude volcanic island arcs (Bayon et al., 2023; Hartmann et al., 2014). We propose that the tropical arc-continent collision starting in the late Miocene resulted in faulting and fracturing of the Luzon Arc, promoting further uplift and exposure. These newly exposed areas then become highly susceptible to weathering, along with heavy rainfall in the tropics, causing high rates of physical and chemical erosion of basaltic rocks in the Luzon Arc. The enhanced weathering inputs from volcanic island arc (mainly the Luzon Arc and the Pro-Philippine Arc) introduced significant radiogenic Nd into the surrounding and Pacific seawaters and then migrated to Site U1501 (Figure 3g). The intermediary of water masses, which carries radiogenic Nd from island arc weathering, explains why the detrital sediment ε_{Nd} records at Site U1501 remain stable, whereas the foraminiferal values exhibit radiogenic trend since 9 Ma (Figure 2). The interpretation is consistent with previous study that the collision of the Australian–Banda–Sunda Arcs over the last 4 Ma was the main source of radiogenic seawater Nd recovered from marine sediment along the northwestern Australian margin, with unradiogenic Nd of detritus (Bayon et al., 2023). Furthermore, the pronounced radiogenic trend in ε_{Nd} values could be buffered by unradiogenic inputs after 3 Ma (Figure 3c), which may be due to an increased influx of detrital sediments from Taiwan Island (ε_{Nd} values of western Taiwan riverine sediments, −14 to −12) to the northern SCS since the late Pliocene (Dou et al., 2016; Wan et al., 2010).

4.3. Mass Balance of Weathering Input From Island Arc Relative to Asian Continent Since 9 Ma

Additionally, we attempt to quantify the contribution of weathering input from the island arc relative to the Asian continent since 9 Ma, using a mass balance approach based on the foraminiferal ε_{Nd} data set at Site U1501. Before 9 Ma, ε_{Nd} values were predominantly influenced by the East Asian Continent weathering input (W) and Pacific deep-water masses (S), expressed by Equation 1:

$$(\varepsilon_{Nd})_W[Nd]_W + (\varepsilon_{Nd})_S[Nd]_S = (\varepsilon_{Nd})_A([Nd]_W + [Nd]_S) \quad (1)$$

After 9 Ma, weathering input from the island arc (I) contributed to the Nd balance, expressed by Equation 2:

$$(\varepsilon_{Nd})_W[Nd]_W + (\varepsilon_{Nd})_S[Nd]_S + (\varepsilon_{Nd})_I[Nd]_I = (\varepsilon_{Nd})_A([Nd]_W + [Nd]_S + [Nd]_I) \quad (2)$$

Here, $(\varepsilon_{Nd})_W$, $(\varepsilon_{Nd})_S$, $(\varepsilon_{Nd})_I$ and $(\varepsilon_{Nd})_A$ correspond to the ε_{Nd} values from the East Asian Continent weathering, seawater masses, island arc weathering and Site U1501. $[Nd]_W$, $[Nd]_S$, and $[Nd]_I$ represent Nd flux, contributing to foraminiferal Nd at Site U1501. We do not follow the conventional method of separately estimating the end-member contributions as Nd fluxes are completely unconstrained within a million-year geological timescale. Instead, we simplify the model by combining the Nd flux and its fractions of the total Nd mass into a single parameter and obtain the relative contribution of island arc versus continental weathering (Yu et al., 2022). Over the last 9 Ma, we obtain $[Nd]_I = 1/11[Nd]_W$ (see Text S3 in Supporting Information S1 for details). In theory, both the reduction of continent weathering input and enhanced island arc weathering input could lead to radiogenic variation in ε_{Nd} at Site U1501. The mass balance result indicates that, in conservative assumptions, injection of the Nd flux of arc island weathering under the long-term decreasing continental weathering input, accounting for 1/11 Nd flux from continental weathering, is sufficient to explain the observed radiogenic ε_{Nd} since 9 Ma. Such results do not demonstrate that the contribution of island arc weathering is small, 1/11 of continental weathering, however, highlight the significant role of island arc in the Nd budget. These findings align with studies highlighting the disproportionately between minor island arcs area and significant contribution to global weathering (Jagoutz et al., 2016). Specifically, weathering of island arcs accounts for approximately 25% of global weathering flux with ~3% of land area (Milliman & Farnsworth, 2011).

4.4. Impact of Western Pacific Island Arc Weathering on Global Cooling Since the Late Miocene

In general, basaltic rocks in warm and wet tropical belts have much higher CO_2 consumption rates than granitic watersheds outside of the tropics, often by two orders of magnitude (Dessert et al., 2001). The continent–island arc collisions have led to the obduction of volcanic island arcs onto continents, creating kilometers-thick ophiolite complexes and increasing the surface area of highly weatherable ultramafic–mafic rocks (Hartmann et al., 2014; Jagoutz et al., 2016). In the context of the warm and humid tropics, this has led to a greatly intensified flux of silicate weathering, ultimately playing an important role in the consumption of atmospheric CO_2 concentrations and triggering global cooling in the past (Macdonald et al., 2019; Park et al., 2020).

Consequently, our new seawater ε_{Nd} records from the northern SCS indicate that weathering of tropical island arc in the context of arc-continent collision has increased substantially over the last 9 Ma. Such results thus provide strong evidence to support the previously proposed hypothesis that orographically driven chemical denudation of western Pacific island arcs could have played an important role in chemical weathering and global cooling since the late Miocene (Bayon et al., 2023; Jagoutz et al., 2016; Macdonald et al., 2019; Park et al., 2020).

In addition, ε_{Nd} records from Site U1501 present cyclic-like oscillations at million-year timescales after the middle Miocene (Figure 2). Orbital forcing generally drives periodic variations in climate systems, involved in seasonal contrasts, precipitation, and chemical weathering (De Vleeschouwer et al., 2020; Pälike et al., 2006). Therefore, the cyclic oscillations in ε_{Nd} records at Site U1501, in the case of real signals, are likely related to changes in weathering input from the continent and island arc, modulated by astronomical forcing. However, the limited resolution of ε_{Nd} data in this study hindered us from identifying reliable orbital solutions. Further study with high-resolution records will be necessary to understand the mechanism of orbital forcing in chemical weathering.

5. Conclusions

The ε_{Nd} values of mixed planktonic foraminifera from IODP Site U1501 in the northern SCS were analyzed and discussed, in order to trace past changes in weathering input and its links with tectonics and climate change. The foraminiferal ε_{Nd} records reveal a more unradiogenic trend between 17 and 9 Ma, which was induced by the progressive isolation of the SCS basin from the Pacific Ocean and intensified weathering inputs from the Asian Continent. In contrast, the markedly more radiogenic ε_{Nd} trend observed since 9 Ma is attributed to the collision between the Luzon Arc and the Eurasian Continent, leading to the rapid weathering of large volumes of radiogenic basaltic rocks under tropical climates. This process may have played an important role in the consumption of atmospheric CO_2 and contributed to global cooling since the late Miocene. In summary, the ε_{Nd} record at Site U1501 demonstrates a dynamic balance of weathering inputs between the East Asian Continent and the Luzon Arc since the late Oligocene, under the control of regional tectonic evolution.

Data Availability Statement

The data are available at Li & Wan (2025).

Acknowledgments
We acknowledge the International Ocean Discovery Program and the scientific party and technicians of IODP Expedition 368 for recovering the samples. We thank the editor, Germain Bayon and one anonymous reviewer for their constructive comments. This work was supported by the National Natural Science Foundation of China (42125602), National Key Research and Development Program of China (2022YFF0800503), National Natural Science Foundation of China (42376055), Strategic Priority Research Program of the Chinese Academy of Sciences (XDB40010100).

References

Abbott, A. N., Haley, B. A., & McManus, J. (2015). Bottoms up: Sedimentary control of the deep North Pacific Ocean's ε_{Nd} signature. *Geology*, *43*(11), 1035. https://doi.org/10.1130/G37114.1

Amakawa, H., Yu, T.-L., Tazoe, H., Obata, H., Gamo, T., Sano, Y., et al. (2019). Neodymium concentration and isotopic composition distributions in the southwestern Indian ocean and the Indian sector of the Southern Ocean. *Chemical Geology*, *511*, 190–203. https://doi.org/10.1016/j.chemgeo.2019.01.007

Bayon, G., Patriat, M., Godderis, Y., Trinquier, A., De Deckker, P., Kulhanek, D. K., et al. (2023). Accelerated mafic weathering in Southeast Asia linked to late neogene cooling. *Science Advances*, *9*(13), 3141. https://doi.org/10.1126/sciadv.adf3141

Burton, K., & Vance, D. (2000). Glacial–interglacial variations in the neodymium isotope composition of seawater in the Bay of Bengal recorded by planktonic foraminifera. *Earth and Planetary Science Letters*, *176*(3–4), 425–441. https://doi.org/10.1016/S0012-821X(00)00011-X

Chen, W.-H., Huang, C.-Y., Lin, Y.-J., Zhao, Q., Yan, Y., Chen, D., et al. (2015). Depleted deep South China Sea $\delta^{13}C$ paleoceanographic events in response to tectonic evolution in Taiwan–Luzon strait since middle Miocene. *Deep Sea Research Part II: Topical Studies in Oceanography*, *122*, 195–225. https://doi.org/10.1016/j.dsr2.2015.02.005

Chen, W.-H., Huang, C.-Y., Yan, Y., Dilek, Y., Chen, D., Wang, M.-H., et al. (2017). Stratigraphy and provenance of forearc sequences in the Lichi Mélange, Coastal Range: Geological records of the active Taiwan Arc–continent collision. *Journal of Geophysical Research: Solid Earth*, *122*(9), 7408–7436. https://doi.org/10.1002/2017JB014378

Clift, P. D. (2006). Controls on the erosion of Cenozoic Asia and the flux of clastic sediment to the ocean. *Earth and Planetary Science Letters*, *241*(3), 571–580. https://doi.org/10.1016/j.epsl.2005.11.028

Clift, P. D., Lee, J. I., Clark, M. K., & Blusztajn, J. (2002). Erosional response of South China to arc rifting and monsoonal strengthening; a record from the South China Sea. *Marine Geology*, *184*(3), 207–226. https://doi.org/10.1016/S0025-3227(01)00301-2

Clift, P. D., Wan, S., & Blusztajn, J. (2014). Reconstructing chemical weathering, physical erosion and monsoon intensity since 25 Ma in the Northern South China Sea: A review of competing proxies. *Earth-Science Reviews*, *130*, 86–102. https://doi.org/10.1016/j.earscirev.2014.01.002

Colin, C., Tisnérat-Laborde, N., Mienis, F., Collart, T., Pons-Branchu, E., Dubois-Dauphin, Q., et al. (2019). Millennial–scale variations of the Holocene North Atlantic Mid–depth gyre inferred from radiocarbon and neodymium isotopes in cold water corals. *Quaternary Science Reviews*, *211*, 93–106. https://doi.org/10.1016/j.quascirev.2019.03.011

Copard, K., Colin, C., Douville, E., Freiwald, A., Gudmundsson, G., De Mol, B., & Frank, N. (2010). Nd isotopes in deep–sea corals in the North–Eastern Atlantic. *Quaternary Science Reviews*, *29*(19), 2499–2508. https://doi.org/10.1016/j.quascirev.2010.05.025

Dessert, C., Dupré, B., François, L. M., Schott, J., Gaillardet, J., Chakrapani, G., & Bajpai, S. (2001). Erosion of Deccan traps determined by river geochemistry: Impact on the global climate and the $^{87}Sr/^{86}Sr$ ratio of seawater. *Earth and Planetary Science Letters*, *188*(3), 459–474. https://doi.org/10.1016/S0012-821X(01)00317-X

De Vleeschouwer, D., Drury, A. J., Vahlenkamp, M., Rochholz, F., Liebrand, D., & Pälike, H. (2020). High–latitude biomes and rock weathering mediate climate–carbon cycle feedbacks on eccentricity timescales. *Nature Communications*, *11*(1), 5013. https://doi.org/10.1038/s41467-020-18733-w

Dou, Y., Yang, S., Shi, X., Clift, P., Liu, S., Liu, J., et al. (2016). Provenance weathering and erosion records in Southern Okinawa trough sediments since 28 ka: Geochemical and Sr-Nd-Pb isotopic evidences. *Chemical Geology*, *425*, 93–109. https://doi.org/10.1016/j.chemgeo.2016.01.029

Dubois-Dauphin, Q., Colin, C., Bonneau, L., Montagna, P., Wu, Q., Van Rooij, D., et al. (2017). Fingerprinting Northeast Atlantic water masses using neodymium isotopes. *Geochimica et Cosmochimica Acta*, *210*, 267–288. https://doi.org/10.1016/j.gca.2017.04.002

Frank, M., Whiteley, N., Kasten, S., Hein, J. R., & O'Nions, K. (2002). North Atlantic deep water export to the Southern Ocean over the past 14 Myr: Evidence from Nd and Pb isotopes in ferromanganese crusts. *Paleoceanography*, *17*(2), 1–9. https://doi.org/10.1029/2000PA000606

Galy, V., France-Lanord, C., Beyssac, O., Faure, P., Kudrass, H., & Palhol, F. (2007). Efficient organic carbon burial in the Bengal fan sustained by the Himalayan erosional system. *Nature*, *450*(7168), 407–410. https://doi.org/10.1038/nature06273

Goldstein, S. J., & Jacobsen, S. B. (1988). Nd and Sr isotopic systematics of river water suspended material: Implications for crustal evolution. *Earth and Planetary Science Letters*, *87*(3), 249–265. https://doi.org/10.1016/0012-821X(88)90013-1

Hall, R. (2002). Cenozoic geological and plate tectonic evolution of SE Asia and the SW Pacific: Computer–based reconstructions, model and animations. *Journal of Asian Earth Sciences*, *20*(4), 353–431. https://doi.org/10.1016/S1367-9120(01)00069-4

Hall, R. (2009). Southeast Asia's changing palaeogeography. *Blumea*, *54*(1–2), 148–161. https://doi.org/10.3767/000651909X475941

Hartmann, J., Moosdorf, N., Lauerwald, R., Hinderer, M., & West, A. J. (2014). Global chemical weathering and associated P–release–The role of lithology, temperature and soil properties. *Chemical Geology*, *363*, 145–163. https://doi.org/10.1016/j.chemgeo.2013.10.025

Herbert, T. D., Dalton, C. A., Liu, Z., Salazar, A., Si, W., & Wilson, D. S. (2022). Tectonic degassing drove global temperature trends since 20 Ma. *Science*, *377*(6601), 116–119. https://doi.org/10.1126/science.abl4353

Holbourn, A., Kuhnt, W., Frank, M., & Haley, B. A. (2013). Changes in Pacific Ocean circulation following the Miocene onset of permanent Antarctic ice cover. *Earth and Planetary Science Letters*, *365*, 38–50. https://doi.org/10.1016/j.epsl.2013.01.020

Huang, C.-Y., Chen, W.-H., Wang, M.-H., Lin, C.-T., Yang, S., Li, X., et al. (2018). Juxtaposed sequence stratigraphy, temporal-spatial variations of sedimentation and development of modern-forming forearc Lichi Mélange in North Luzon trough forearc basin onshore and offshore Eastern Taiwan: An overview. *Earth-Science Reviews*, *182*, 102–140. https://doi.org/10.1016/j.earscirev.2018.01.015

Jagoutz, O., Macdonald, F. A., & Royden, L. (2016). Low–latitude arc–continent collision as a driver for global cooling. *Proceedings of the National Academy of Sciences of the United States of America*, *113*(18), 4935–4940. https://doi.org/10.1073/pnas.1523667113

Jeandel, C., Arsouze, T., Lacan, F., Téchiné, P., & Dutay, J.-C. (2007). Isotopic Nd compositions and concentrations of the lithogenic inputs into the ocean: A compilation, with an emphasis on the margins. *Chemical Geology*, *239*(1), 156–164. https://doi.org/10.1016/j.chemgeo.2006.11.013

Jian, Z., Dang, H., Yu, J., Wu, Q., Gong, X., Stepanek, C., et al. (2023). Changes in deep Pacific circulation and carbon storage during the Pliocene–Pleistocene transition. *Earth and Planetary Science Letters*, *605*, 118020. https://doi.org/10.1016/j.epsl.2023.118020

Jian, Z., Jin, H., Kaminski, M. A., Ferreira, F., Li, B., & Yu, P.-S. (2019). Discovery of the marine Eocene in the Northern South China Sea. *National Science Review*, *6*(5), 881–885. https://doi.org/10.1093/nsr/nwz084

Jian, Z., Larsen, H. C., & Alvarez Zarikian, C. A. (2018). Testing hypotheses for lithosphere thinning during continental breakup: Drilling at the South China Sea rifted margin. In *International Ocean Discovery Program Expedition 368 Preliminary Report, 368* (pp. 1–30). https://doi.org/10.14379/iodp.pr.368.2018

Jin, H., Wan, S., Clift, P. D., Liu, C., Huang, J., Jiang, S., et al. (2022). Birth of the Pearl River at 30 Ma: Evidence from sedimentary records in the Northern South China Sea. *Earth and Planetary Science Letters*, *600*, 117872. https://doi.org/10.1016/j.epsl.2022.117872

Jin, H., Wan, S., Liu, C., Zhao, D., Pei, W., Yu, Z., et al. (2023). Evolution of silicate weathering in South China since 30 Ma: Controlling factors and global implications. *Global and Planetary Change*, *223*, 104095. https://doi.org/10.1016/j.gloplacha.2023.104095

Kawabe, M., & Fujio, S. (2010). Pacific Ocean circulation based on observation. *Journal of Oceanography*, *66*(3), 389–403. https://doi.org/10.1007/s10872-010-0034-8

Kender, S., Bogus, K. A., Cobb, T. D., & Thomas, D. J. (2018). Neodymium evidence for increased circumpolar deep water flow to the North Pacific during the middle Miocene climate transition. *Paleoceanography and Paleoclimatology*, *33*(7), 672–682. https://doi.org/10.1029/2017PA003309

Lacan, F., & Jeandel, C. (2005). Neodymium isotopes as a new tool for quantifying exchange fluxes at the continent–ocean interface. *Earth and Planetary Science Letters*, *232*(3), 245–257. https://doi.org/10.1016/j.epsl.2005.01.004

Lacan, F., Tachikawa, K., & Jeandel, C. (2012). Neodymium isotopic composition of the oceans: A compilation of seawater data. *Chemical Geology*, *300*, 177–184. https://doi.org/10.1016/j.chemgeo.2012.01.019

Le Houedec, S., Meynadier, L., & Allègre, C. J. (2016). Seawater Nd isotope variation in the western Pacific Ocean since 80 Ma (ODP 807, Ontong Java Plateau). *Marine Geology*, *380*, 138–147. https://doi.org/10.1016/j.margeo.2016.07.005

Li, M., & Wan, S. (2025). Northern South China sea planktonic foraminifera eNd from IODP site U1501 [Dataset]. In *Tectonics modulated long-term weathering inputs from the East Asian continent and tropical Island Arc to the South China Sea Since the late Oligocene*. Zenodo. https://doi.org/10.5281/zenodo.15349177

Lin, A. T., Watts, A. B., & Hesselbo, S. P. (2003). Cenozoic stratigraphy and subsidence history of the South China Sea margin in the Taiwan region. *Basin Research*, *15*(4), 453–478. https://doi.org/10.1046/j.1365-2117.2003.00215.x

Ling, H. F., Burton, K. W., O'Nions, R. K., Kamber, B. S., von Blanckenburg, F., Gibb, A. J., & Hein, J. R. (1997). Evolution of Nd and Pb isotopes in Central Pacific seawater from ferromanganese crusts. *Earth and Planetary Science Letters*, *146*(1–2), 1–12. https://doi.org/10.1016/S0012-821X(96)00224-5

Liu, Z., Zhao, Y., Colin, C., Stattegger, K., Wiesner, M. G., Huh, C.-A., et al. (2016). Source-to-sink transport processes of fluvial sediments in the South China Sea. *Earth-Science Reviews*, *153*, 238–273. https://doi.org/10.1016/j.earscirev.2015.08.005

Ma, X., Tian, J., Ma, W., Li, K., & Yu, J. (2018). Changes of deep Pacific overturning circulation and carbonate chemistry during middle Miocene East Antarctic ice sheet expansion. *Earth and Planetary Science Letters*, *484*, 253–263. https://doi.org/10.1016/j.epsl.2017.12.002

Macdonald, F. A., Swanson-Hysell, N. L., Park, Y., Lisiecki, L., & Jagoutz, O. (2019). Arc–continent collisions in the tropics set Earth's climate state. *Science*, *364*(6436), 181–184. https://doi.org/10.1126/science.aav5300

McKinley, C. C., Thomas, D. J., LeVay, L. J., & Rolewicz, Z. (2019). Nd isotopic structure of the Pacific Ocean 40–10 Ma, and evidence for the reorganization of deep North Pacific Ocean circulation between 36 and 25 Ma. *Earth and Planetary Science Letters*, *521*, 139–149. https://doi.org/10.1016/j.epsl.2019.06.009

Mesalles, L., Mouthereau, F., Bernet, M., Chang, C.-P., Lin, A. T.-S., Fillon, C., & Sengelen, X. (2014). From submarine continental accretion to arc–continent orogenic evolution: The thermal record in southern Taiwan. *Geology*, *42*(10), 907–910. https://doi.org/10.1130/G35854.1

Milliman, J. D., & Farnsworth, K. L. (2011). *River discharge to the coastal ocean: A global synthesis*. Cambridge University Press.

Molnar, P., & Cronin, T. W. (2015). Growth of the maritime continent and its possible contribution to recurring ice ages. *Paleoceanography*, *30*(3), 196–225. https://doi.org/10.1002/2014PA002752

Pälike, H., Norris, R. D., Herrle, J. O., Wilson, P. A., Coxall, H. K., Lear, C. H., et al. (2006). The heartbeat of the Oligocene climate system. *Science*, *314*(5807), 1894–1898. https://doi.org/10.1126/science.1133822

Park, Y., Maffre, P., Goddéris, Y., Macdonald, F. A., Anttila, E. S. C., & Swanson-Hysell, N. L. (2020). Emergence of the Southeast Asian islands as a driver for neogene cooling. *Proceedings of the National Academy of Sciences of the United States of America*, *117*(41), 25319–25326. https://doi.org/10.1073/pnas.2011033117

Piepgras, D. J., & Wasserburg, G. J. (1982). Isotopic composition of neodymium in waters from the Drake Passage. *Science*, *217*(4556), 207–214. https://doi.org/10.1126/science.217.4556.207

Piotrowski, A. M., Galy, A., Nicholl, J. A. L., Roberts, N., Wilson, D. J., Clegg, J. A., & Yu, J. (2012). Reconstructing deglacial North and South Atlantic deep water sourcing using foraminiferal Nd isotopes. *Earth and Planetary Science Letters*, *357–358*, 289–297. https://doi.org/10.1016/j.epsl.2012.09.036

Qu, T., Du, Y., & Sasaki, H. (2006). South China Sea throughflow: A heat and freshwater conveyor. *Geophysical Research Letters*, *33*(23). https://doi.org/10.1029/2006GL028350

Raymo, M. E., & Ruddiman, W. F. (1992). Tectonic forcing of late Cenozoic climate. *Nature*, *359*(6391), 117–122. https://doi.org/10.1038/359117a0

Sajona, F. G., Maury, R. C., Pubellier, M., Leterrier, J., Bellon, H., & Cotten, J. (2000). Magmatic source enrichment by slab-derived melts in a young post-collision setting, central Mindanao (Philippines). *Lithos*, *54*(3), 173–206. https://doi.org/10.1016/S0024-4937(00)00019-0

Scher, H. D., & Martin, E. E. (2004). Circulation in the Southern Ocean during the paleogene inferred from neodymium isotopes. *Earth and Planetary Science Letters*, *228*(3), 391–405. https://doi.org/10.1016/j.epsl.2004.10.016

Shen, X., Wan, S., France-Lanord, C., Clift, P. D., Tada, R., Révillon, S., et al. (2017). History of Asian eolian input to the Sea of Japan since 15 Ma: Links to Tibetan uplift or global cooling? *Earth and Planetary Science Letters*, *474*, 296–308. https://doi.org/10.1016/j.epsl.2017.06.053

Shu, W., Colin, C., Liu, Z., & Dapoigny, A. (2024). Late Oligocene–Miocene evolution of deep-water circulation in the abyssal South China Sea: Insights from Nd isotopes of fossil fish teeth. *Geology*, *52*(8), 620–624. https://doi.org/10.1130/G52042.1

Sibuet, J.-C., & Hsu, S.-K. (2004). How was Taiwan created? *Tectonophysics*, *379*(1), 159–181. https://doi.org/10.1016/j.tecto.2003.10.022

Sibuet, J.-C., Hsu, S.-K., Le Pichon, X., Le Formal, J.-P., Reed, D., Moore, G., & Liu, C.-S. (2002). East Asia plate tectonics since 15 Ma: Constraints from the Taiwan region. *Tectonophysics*, *344*(1), 103–134. https://doi.org/10.1016/S0040-1951(01)00202-5

Siddall, M., Khatiwala, S., van de Flierdt, T., Jones, K., Goldstein, S. L., Hemming, S., & Anderson, R. F. (2008). Towards explaining the Nd paradox using reversible scavenging in an ocean general circulation model. *Earth and Planetary Science Letters*, *274*(3), 448–461. https://doi.org/10.1016/j.epsl.2008.07.044

Singh, S. P., Singh, S. K., Goswami, V., Bhushan, R., & Rai, V. K. (2012). Spatial distribution of dissolved neodymium and ε_{Nd} in the Bay of Bengal: Role of particulate matter and mixing of water masses. *Geochimica et Cosmochimica Acta*, *94*, 38–56. https://doi.org/10.1016/j.gca.2012.07.017

Solidum, R. U., Castillo, P. R., & Hawkins, J. W. (2003). Geochemistry of lavas from Negros Arc, west central Philippines: Insights into the contribution from the subducting slab. *Geochemistry, Geophysics, Geosystems*, *4*(10). https://doi.org/10.1029/2003GC000513

Song, Z., Wan, S., Colin, C., France-Lanord, C., Yu, Z., Dapoigny, A., et al. (2023). Enhanced weathering input from South Asia to the Indian Ocean since the late Eocene. *Science Bulletin*, *68*(3), 305–313. https://doi.org/10.1016/j.scib.2023.01.015

Tachikawa, K., Athias, V., & Jeandel, C. (2003). Neodymium budget in the modern ocean and paleo–oceanographic implications. *Journal of Geophysical Research*, *108*(C8), 3254. https://doi.org/10.1029/1999JC000285

Tachikawa, K., Piotrowski, A. M., & Bayon, G. (2014). Neodymium associated with foraminiferal carbonate as a recorder of seawater isotopic signatures. *Quaternary Science Reviews*, *88*, 1–13. https://doi.org/10.1016/j.quascirev.2013.12.027

Tanaka, T., Togashi, S., Kamioka, H., Amakawa, H., Kagami, H., Hamamoto, T., et al. (2000). JNdi–1: A neodymium isotopic reference in consistency with LaJolla neodymium. *Chemical Geology*, *168*(3), 279–281. https://doi.org/10.1016/S0009-2541(00)00198-4

vande Flierdt, T., Frank, M., Halliday, A. N., Hein, J. R., Hattendorf, B., Günther, D., & Kubik, P. W. (2004). Deep and bottom water export from the Southern Ocean to the Pacific over the past 38 million years. *Paleoceanography*, *19*(1), PA1020. https://doi.org/10.1029/2003PA000923

Wan, S., Li, A., Clift, P. D., & Stuut, J.-B. W. (2007). Development of the East Asian monsoon: Mineralogical and sedimentologic records in the northern South China Sea since 20 Ma. *Palaeogeography, Palaeoclimatology, Palaeoecology*, *254*(3), 561–582. https://doi.org/10.1016/j.palaeo.2007.07.009

Wan, S., Li, A., Clift, P. D., Wu, S., Xu, K., & Li, T. (2010). Increased contribution of terrigenous supply from Taiwan to the Northern South China Sea since 3 Ma. *Marine Geology*, *278*(1), 115–121. https://doi.org/10.1016/j.margeo.2010.09.008

Wei, G., Liu, Y., Ma, J., Xie, L., Chen, J., Deng, W., & Tang, S. (2012). Nd, Sr isotopes and elemental geochemistry of surface sediments from the South China Sea: Implications for Provenance Tracing. *Marine Geology*, *319*, 21–34. https://doi.org/10.1016/j.margeo.2012.05.007

Westerhold, T., Marwan, N., Drury, A. J., Liebrand, D., Agnini, C., Anagnostou, E., et al. (2020). An astronomically dated record of Earth's climate and its predictability over the last 66 million years. *Science*, *369*(6509), 1383–1387. https://doi.org/10.1126/science.aba6853

Wu, Q., Colin, C., Liu, Z., Bassinot, F., Dubois-Dauphin, Q., Douville, E., et al. (2017). Foraminiferal ε_{Nd} in the deep North–Western Subtropical Pacific Ocean: Tracing changes in weathering input over the last 30,000 years. *Chemical Geology*, *470*, 55–66. https://doi.org/10.1016/j.chemgeo.2017.08.022

Wu, Q., Colin, C., Liu, Z., Douville, E., Dubois-Dauphin, Q., & Frank, N. (2015). New insights into hydrological exchange between the South China Sea and the Western Pacific Ocean based on the Nd isotopic composition of seawater. *Deep Sea Research Part II: Topical Studies in Oceanography*, *122*, 25–40. https://doi.org/10.1016/j.dsr2.2015.11.005

Wyrtki, K. (1961). *Physical oceanography of the Southeast Asian waters* (Vol. 2). University of California, Scripps Institution of Oceanography.

Yang, Y., Galy, A., Fang, X., Yang, R., Zhang, W., Song, B., et al. (2021). Neodymium isotopic constraints on Cenozoic Asian dust provenance changes linked to the exhumation history of the Northern Tibetan Plateau and the Central Asian Orogenic Belt. *Geochimica et Cosmochimica Acta*, *296*, 38–55. https://doi.org/10.1016/j.gca.2020.12.026

Yu, Z., Colin, C., Ma, R., Meynadier, L., Wan, S., Wu, Q., et al. (2018). Antarctic intermediate water penetration into the Northern Indian Ocean during the last deglaciation. *Earth and Planetary Science Letters*, *500*, 67–75. https://doi.org/10.1016/j.epsl.2018.08.006

Yu, Z., Colin, C., Meynadier, L., Douville, E., Dapoigny, A., Reverdin, G., et al. (2017). Seasonal variations in dissolved neodymium isotope composition in the Bay of Bengal. *Earth and Planetary Science Letters*, *479*, 310–321. https://doi.org/10.1016/j.epsl.2017.09.022

Yu, Z., Colin, C., Wilson, D. J., Bayon, G., Song, Z., Sepulcre, S., et al. (2022). Millennial variability in intermediate ocean circulation and Indian monsoonal weathering inputs during the last Deglaciation and Holocene. *Geophysical Research Letters*, *49*(21), e2022GL100003. https://doi.org/10.1029/2022GL100003